Z. Phys. C - Particles and Fields 16, 217-228 (1983)

Zeitschrift für Physik C Particles and Fields

Properties of Gluon Jets

L.M. Jones[1] and R. Migneron[2, 3]

Deutsches Elektronen-Synchrotron DESY, D-2000 Hamburg, Federal Republic of Germany

Received 18 June 1982

Abstract. We compute the expected properties of gluon jets in a model based on the KUV jet calculus and recombination. Emphasis is placed on a) the production of baryons, and b) the question of whether hadrons produced by the decays of Zweig rule stable quarkonia (e.g. the upsilon) in e^+e^- have markedly different energy spectra from those produced by the adjacent quark-antiquark continuum.

I. Introduction

One of the important questions in current jet phenomenology is whether jets produced by gluons are distinguishable in the laboratory from those produced by quarks. Although jet calculus indicates that the multiplicity of elementary partons in a gluon jet should be roughly twice that in a quark jet [1], to date there have been few indications that this relation for the multiplicities carries over to the hadrons produced when these partons become confined.

By observing the hadrons "on" and "off" resonances which are believed to decay via a three gluon intermediate state, one might hope to isolate the gluon jets. At times, such observations have led to speculations that the gluons do indeed have different properties; in particular it has been proposed that they may be particularly effective in producing baryons [2] (see, however, the later results of [3]), or that their relative effectiveness in producing baryons may have a different x dependence than expected [4]. Other methods have also been used to isolate gluon jets [5].

Various calculations have appeared in the literature which address these questions in different models. An excellent review of baryon production in e^+e^- annihilation can be found in the talk by Gutbrod [6]. In addition to numerous papers using cascade-type integral equations [7], there are various more detailed models. The Lund group [8] have a model in which diquark-antidiquark pairs are created by a tunnelling process. They find that the probability to have a p or $\bar{p}$ as fastest charged particle is slightly greater in a gluon jet than in a quark jet, and that a higher baryon fraction should be produced on the "onia" resonances than off them (but this difference should be less pronounced at higher energies). Meyer [9] uses a more phenomenological but rather similar approach in which quark-antiquark pairs are created and align with other quarks to make baryons.

The work of Hoffmann [10] uses a weighted phase space to generate the distribution of quarks within the jets, and the recombination model to produce baryons and mesons from them. He finds that the fraction of baryons is augmented by 30–45% in Υ decays as compared to $q\bar{q}$ jets, and that the distribution in x of both protons and mesons is steeper on the Υ than off it.

Recently we have been exploring a model for jet fragmentation which utilizes the Konishi-Ukawa-Veneziano (KUV) [1] jet calculus (to produce the partons in the jet) and the recombination model (to stick them together into mesons or baryons). Results of the procedure for the e^+e^- continuum annihiliation into quark-antiquark pairs are contained in our previous papers [11, 12] along with discussion and rationalizations. In this paper we apply the same method to the gluon jets, and we compute the spectrum for baryons and mesons "on" and "off" the upsilon and toponium resonances. Our results turn out to be very similar to those of Hoffmann,

1 Permanent address: Physics Department, 1110 West Green St. Urbana, IL 61801, USA

2 Permanent address: Dept. of Applied Mathematics, University of Western Ontario, London, Ontario, N6A5B9, Canada

3 Supported in part by the NSERC of Canada

0170-9739/83/0016/0217/$02.40

despite the difference in method for producing the parton distribution in the jets.

A brief summary of our basic formulae is given in Sect. II. In Sect. III we display the basic properties of the fragmentation functions for gluons into baryons, pions and kaons and compare with quark jet fragmentation functions. In Sect. IV we compare the expected energy spectra (per event) of baryons and mesons "on" and "off" the presently available upsilon resonance and the expected top quark resonance (which we have assumed for purposes of calculation to be at 42 GeV). Finally Sect. V contains conclusions and summary.

In three Appendices we provide additional discussion and comparison with data. Appendix A shows the relative sizes of the baryon and meson predictions; Appendix B compares our parameterization with available meson data; and Appendix C discusses some technical details, including the relation of our work to a previous calculation by Eilam and Zahir [25] of the quark and gluon fragmentation into baryons.

II. Methods

Jet Calculus

As in [12], our technique for the baryon production is to compute the three parton spectrum of the jet using the KUV formula (see Fig. 1)

$$D_{a_1a_2a_3,i}(x_1,x_2,x_3;Q^2)=\sum_{jb_1b_2c_1c_2b_2'}\int_{Y_0}^{Y}dy\int_{Y_0}^{y}dy'$$
$$\cdot\int dx\,dz\,dz'\,dx''\,dx'\,dw_1\,dw_2\,dw_3 D_{a_1b_1}(w_1,y-Y_0)$$
$$\cdot D_{a_2c_1}(w_2,y'-Y_0)D_{a_3c_2}(w_3,y'-Y_0)\hat{P}_{b_2'\to c_1c_2}(z')$$
$$\cdot D_{b_2'b_2}(x'',y-y')\hat{P}_{j\to b_1b_2}(z)D_{ji}(x,Y-y)$$
$$\cdot\delta(x_1-w_1zx)\delta(x_2-z'x'w_2)\,.$$
$$\cdot\delta[x_3-(1-z')x'w_3]\delta[x'-x''x(1-z)] \qquad (2.1)$$

where

$$Y=\frac{1}{2\pi b}\ln[1+\alpha_0 b\ln Q^2/\Lambda^2]; \qquad 12\pi b=11N_c-2N_f$$

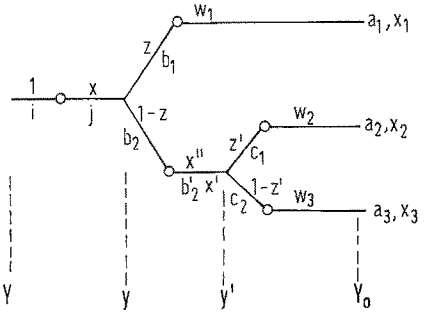

Fig. 1. Diagrammatic version of (2.1) for the three parton inclusive distribution

with

$$\alpha_s=\frac{1}{b\ln(Q^2/\Lambda'^2)}; \qquad \Lambda'^2=\Lambda^2 e^{-1/(b\alpha_0)}$$

and x_1, x_2, and x_3 are the energy fractions of the three partons under consideration. (α_0 is the strength of the strong coupling at $Q^2=\Lambda^2$. We take $\alpha_0=10$ throughout.) This allows for evolution of the jet from a large Q^2 down to a last branching when partons reach "off shellness" Q_0^2.

At Q_0 we prepare for the hadronization by splitting all the gluons into quark-antiquark pairs according to the Chang-Hwa method [13].

$$\bar{P}_{g\to q\bar{q}}(z)=\frac{3}{2N_f}[z^2+(1-z)^2]. \qquad (2.2)$$

All the quark triplets of the appropriate flavors are then recombined into a baryon at x using the recombination probability

$$R_B\frac{x_1x_2x_3}{x^3}\delta(x_1+x_2+x_3-x). \qquad (2.3)$$

The overall fragmentation function than has 4 basic components: $3q$, when the three partons of (2.1) are all quarks; $2q+g$ when one is a gluon and this is converted using (2.2) prior to the recombination, $2g+q$ and $3g$.

For the mesons, exactly the same procedure is followed except that quark-antiquark sets are created, and the recombination function used is

$$R_M\frac{x_1x_2}{x^2}\delta(x_1+x_2-x). \qquad (2.4)$$

In (2.3) and (2.4) R_B and R_M are constants whose values are discussed in Sect. III and Appendix B.

Because our recombination functions contain only integer powers of the x_i, we find it straightforward to compute the moments of the recombined fragmentation functions, as explained in [11] and [12]. These moments are then inverted using the method of Yndurain [14]. Due to difficulties in obtaining sufficient numerical accuracy for this technique for large moments, we have limited our study to meson spectra produced by the second through 14th moments. For the baryons, we use moments between 3 and 11; in this case larger moments require so many jet calculus terms that they become difficult to fit in the computer.

We have computed all the terms in the jet calculus expression and have not approximated any of the pieces.

Quarkonium Decay Spectra

To obtain the baryon energy spectrum per event at the upsilon and toponium resonances, we have taken

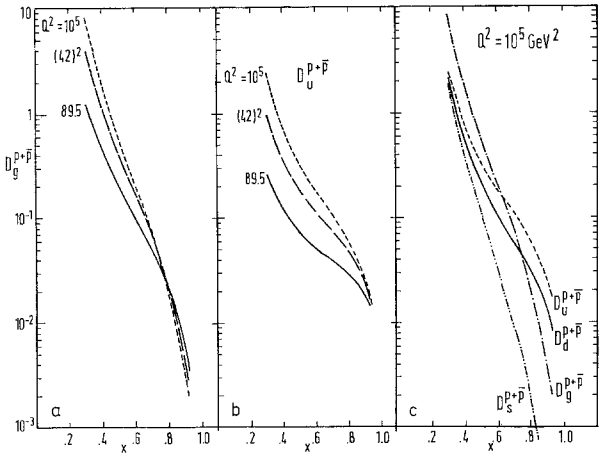

Fig. 2a–c. Jet fragmentation functions into proton plus anti-proton. All curves were computed using the parameters $Q_0^2=2$ GeV^2, $\Lambda=0.2$ GeV, and $R_B=27/4$. **a** Dependence on Q^2 of the gluon fragmentation function into proton plus antiproton. **b** dependence on Q^2 of the up quark fragmentation function into proton plus antiproton. **c** comparison at $Q^2=10^5$ of the various possible fragmentation functions into proton plus antiproton

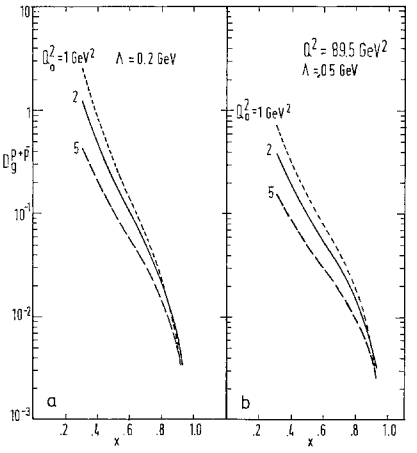

Fig. 3a and b. Behavior of the gluon fragmentation function into proton plus antiproton at $Q^2=89.5$ GeV^2 (the upsilon). All curves were computed with $R_B=27/4$. Here we show the dependence on the parameters Q_0^2 and Λ in the jet calculus expressions. **a** $\Lambda=200$ MeV; **b** $\Lambda=50$ MeV

the probability for decay into three gluon jets [15]

$$\frac{1}{\Gamma_{3g}}\frac{d\Gamma}{dx_1\,dx_2\,dx_3}=\frac{1}{\pi^2-9}\cdot\delta(x_1+x_2+x_3-2)\cdot\left\{\frac{x_1^2(1-x_1)^2+x_2^2(1-x_2)^2+x_3^2(1-x_3)^2}{x_1^2x_2^2x_3^2}\right\} \tag{2.5}$$

multiplied by the probability for a gluon at x_1 to produce a baryon at x

$$\int d\bar{x}_1 D_g^{p+\bar{p}}(\bar{x}_1,Q^2)\,\delta(x-\bar{x}_1x_1) \tag{2.6}$$

multiplied by 3 to allow for each of the jets to produce a baryon, and integrated over the allowed phase space:

$$\frac{1}{\sigma}\frac{d\sigma}{dx}=3\int d\bar{x}_1\int dx_1dx_2dx_3\,\frac{1}{\Gamma_{3g}}\frac{d\Gamma}{dx_1dx_2dx_3}\cdot D_g^{p+\bar{p}}(\bar{x}_1,Q^2)\,\delta(x-\bar{x}_1x_1). \tag{2.7}$$

In Sect. IV these spectra are compared with the per event spectra calculated at the resonance energy using the quark-antiquark jet program of [11] and [12].

We should mention that in these applications the Q^2 of all jets (i.e. the three gluon jets in the case of the quarkonia and the two quark jets in the case of the continuum) has been taken in all calculations to be equal to the center of mass energy squared of the entering e^+e^- system. While there is some justification for this in the case of the $e^+e^-\to q\bar{q}$ reactions (it has been shown that there is a gauge in which there is only one jet, with off-shellness Q^2 [16]), there is no clear-cut choice for the three-gluon decays. Some idea of the dependence of the answers on a different choice of Q^2 can be obtained from Fig. 2.

III. Raw Jet Fragmentation Functions

Baryon Production

From the formulae in Sect. II we obtain the gluon jet fragmentation functions into proton+antiproton shown in Figs. 2–4. The dependence on the Q^2 of the jet is shown in Fig. 2a; for comparison we show in Fig. 2b the Q^2 dependence of the fragmentation function for the up quark into the same final state, and in Fig. 2c the relative sizes of fragmentation functions of various partons into baryons. Notice that the gluon jet reaches its "asymptotic" Altarelli-Parisi behavior earlier in Q^2 than the up quark jet. As we explain in our previous papers [11, 12] this dependence is strongly dependent on the parameters Q_0^2 and Λ used in the evaluation of the jet calculus.

In Fig. 3 we show the dependence of the gluon fragmentation function on the parameters Λ and Q_0 at $Q^2=89.5$ GeV^2. This is similar to the behavior of the quark fragmentation functions shown in [12]. As discussed there, we choose to limit our considerations to small values of Λ near 100 MeV because of recent fits to the scale breaking behavior of the deep inelastic structure functions. Also we limit our considerations for Q_0^2 to relatively small values larger than the mass of the proton (to allow for the possibility of the "intrinsic" fragmentation term discussed in [12]). In the rest of this paper we have used the values $\Lambda=0.2$ GeV and $Q_0^2=2$ GeV^2 for all baryon calculations.

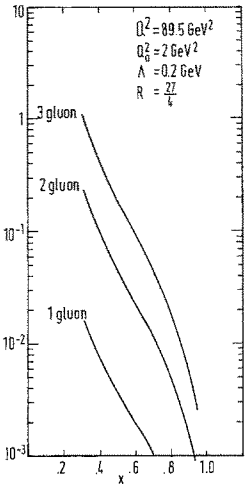

Fig. 4. Decomposition of the gluon fragmentation function in Fig. 1a) into proton plus antiproton. We see that at this Q^2 most of the contribution comes from those jet calculus terms in which three gluons are produced ($Q^2=89.5\ GeV^2$, $Q_0^2=2\ GeV^2$, $\Lambda=0.2\ GeV$, $R_B=27/4$). At very large Q^2, this is no longer true

Figure 4 contains the decomposition into the various contributions: three gluon (with all gluons converted into quark antiquark pairs according to the recipe of (2.2)), two gluon, etc. We note that the three gluon contribution dominates at all x. Although at first this may appear different from the behavior shown in [12], it is in fact similar: at large x the contribution is dominated by the original gluon plus two radiated gluons, whereas at small x the radiated gluons dominate. Both these possibilities are contained in the three gluon contribution. However, the gluon jet curve is steeper than the quark jet curve (see Fig. 2c) because the quark coming from the "leading" gluon does not get all its momentum; hence the produced baryons tend to come out at smaller x.

At very large Q^2, the two gluon and one gluon terms dominate the three gluon term at large x. Asymptotically, therefore, the jet can produce enough quarks at large x to overwhelm those coming from the gluon splitting.

In all these curves and those to follow, we have set the normalization parameter R_B of (2.3) equal to 27/4 for the baryon spectrum analysis. As we discussed in [12] the maximum value allowed by probability arguments [17] would be 27 (the corresponding value for the mesons would be 4), and the expected value would be this divided by some number between 2 and 4 (to allow for the possibility of resonance and meson formation). These arguments were shown to be consistent with the observed size of J/Ψ decay into $p+\bar{p}$ [18]. In the present paper the factor 4 is suggested by the following arguments:

- If all recombination probabilities are divided by 4, this allows roughly for equal chances to form baryons and mesons, and equal chances to form the ground states and the higher excited states. If we had nothing else to go on, this would at least be a reasonable guess.
- For the mesons, dividing by a factor 4 in fact works fairly well. This is shown in Appendix B, where we display calculations of the pion and kaon production in e^+e^- scattering compared with the data.
- Dividing by a factor 4 gives baryon cross sections in e^+e^- scattering of approximately the right size relative to the mesons. This is shown in Appendix A, where we compare our calculations of pion, kaon and proton production in e^+e^- scattering. This is to be compared with the data of [19] which shows π^{+-}, π^0, K^0, and Λ production. Data from protons at large x is not available. When it becomes available the exact value of R_B can be adjusted slightly.

The production of lambdas in gluon jets is exactly proportional to the production of protons, unlike the case of quark jets shown in [12]. If we use exactly the same arguments presented there, ignoring $SU(3)$ breaking, there would be twice as many lambdas as first generation protons in the jet. Allowing for $SU(3)$ breaking, we expect this factor to be reduced by a factor of 2 to 3. This would give roughly equal numbers of lambdas and "elementary" protons produced; this is more or less what is seen at the upsilon [3].

Meson Production

For the calculation of gluon fragmentation functions into mesons we use $R_M=1$, $\Lambda=0.2\ GeV$ (this should be the same everywhere) and $Q_0^2=0.2\ GeV^2$. As shown in Appendix B these fit the presently available data reasonably well. The small value of Q_0 is chosen to reproduce the apparent scale invariance of the data in the presently available energy range. It is still large enough to allow for an "intrinsic" fragmentation of the partons at the end of the chain into pions, although it is a bit small for kaons.

Because of this parametrization, the gluon jets are also more "asymptotic" in this case, as evidenced by the behavior in Figs. 5a and b. The assumption of $SU(3)$ invariance for the quark flavors leads to the fact that Fig. 5a depicts both the neutral kaon and the charged pion fragmentation functions. As usual, there will be corrections due to the mass of the strange quark which alter this result; but the number of neutral kaons should not be much more than a factor two smaller than the number of charged pions, at each x.

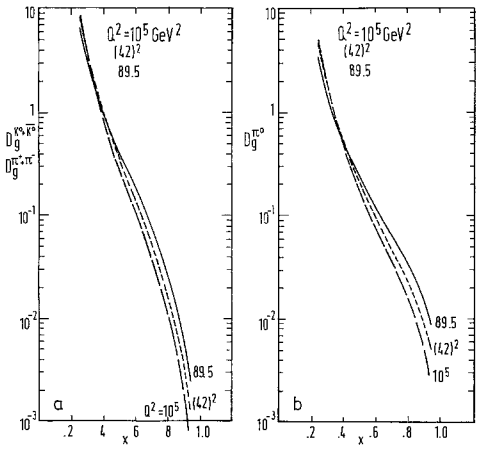

Fig. 5a and b. Dependence on Q^2 of the gluon fragmentation into mesons. All these curves are calculated with $Q_0^2=0.2$ GeV^2, $\Lambda=0.2$ GeV, and $R_M=1$. **a** Production of $K^0+\bar{K}^0$, equal to $\pi^+ + \pi^-$ in the approximations used here; **b** production of neutral pions

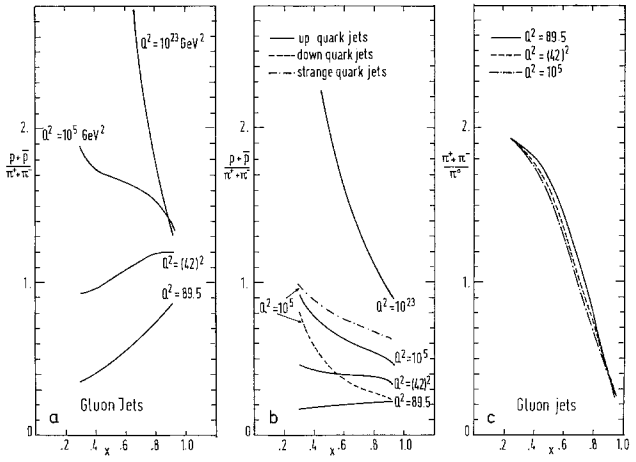

Fig. 6a–c. Particle ratios in the jets using the parametrization of Figs. 2 and 5. **a** Protons to pions in gluon jets; **b** protons to pions in quark jets; **c** charged to neutral pions in gluon jets

Particle Ratios

As discussed by Schierholz and Teper [4], the baryon/meson ratio in gluon jets may be flat or even increasing in presently available data, whereas one might expect it to be a decreasing function of x based on counting rule arguments for the fragmentation functions. In Fig. 6a we display this ratio as a function of Q^2 using the baryon and meson parametrizations discussed above (see Figs. 1, 4). Notice that the x dependence changes as a function of Q^2, due to the fact that at presently accessible energies our parametrization for the baryons is much less asymptotic than the one for the mesons. For those who insist on seeing the asymptotic behavior, we also present in Figs. 6a and b the results at $Q^2=10^{23}$. At this large value, the baryon to meson ratio does decrease as x approaches 1, although it does not have exactly the $(1-x)^2$ behavior mentioned by Schierholz and Teper.

In Fig. 6b we show the same ratio for up quark jets. The qualitative change with Q^2 from a possible rise near $x=1$ to rapid decrease near this point also occurs here, but at small Q^2 there is less of a rise than for the gluon jets. Some sample values for down and strange quark jets are also shown.

One possible difficulty with our approach is displayed in Fig. 6c, which shows the ratio of charged to neutral pions in the gluon jets, as a function of x. This is different from the behavior in quark jets. As can be seen in Fig. 11, the calculations for e^+e^- annihilation produce a neutral pion spectrum which is almost exactly half the charged pion spectrum at all x values. In the gluon jet case, the allowed vertex in which a gluon can split into a $u\bar{u}$ or $d\bar{d}$ quark pair produces low order graphs which can contribute to the π^0 spectrum at large x; and these graphs have no exact counterpart in the charged pion calculation.

We regard the behavior shown in Fig. 6c to be very unlikely. It would not be present in improved jet calculus models [16, 20] where colorless clusters are produced by preconfinement and these colorless, chargeless, clusters decay in some phenomenological way. Its appearance here is, we feel, an artifact of the jet calculus approximation neglecting transverse momentum. Nevertheless, it would be nice to have an experimental check on this point.

IV. Quarkonium Decays

We can now produce the x spectrum of particles produced at the decay op the upsilon and toponium resonances by inserting the gluon jet spectra found in the preceeding section into (2.7). To have a simple means of comparing the situation on and off the resonances, we present the expected spectra per event (dividing out the very different on-resonance and continuum total cross sections).

Our results are presented in Figs. 7–10. We see from Fig. 7 that the answer to the question "are there more baryons per event on or off the resonance" depends to some extent whether one is looking at fast or slow baryons. At the upsilon, for instance, there will be more slow baryons on the resonance and more fast baryons in the continuum surrounding it. At the toponium, the dominance of fast baryons from the 3 gluon jets on resonance is less marked, but there still are more fast baryons in the continuum.

Unfortunately, it is very difficult for us to compare with the numbers quoted in the 1981 Bonn

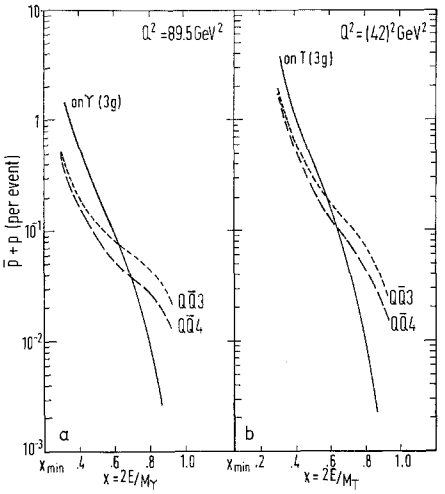

Fig. 7a and b. Protons plus antiprotons per event, on and off the quarkonium resonances. All curves are calculated with $Q_0^2 = 2\,\mathrm{GeV}^2$, $\Lambda = 0.2\,\mathrm{GeV}$, and $R_B = 27/4$. The possibilities $Q\bar{Q}3$ and $Q\bar{Q}4$ for the continuum are discussed in the text. **a** Upsilon; **b** toponium

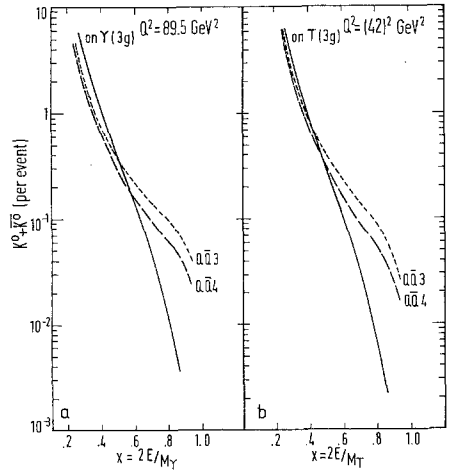

Fig. 8. Neutral kaons per event, on and off the quarkonium resonances. All curves are calculated with $Q_0^2 = 2\,\mathrm{GeV}^2$, $\Lambda = 0.2\,\mathrm{GeV}$, and $R_M = 1$

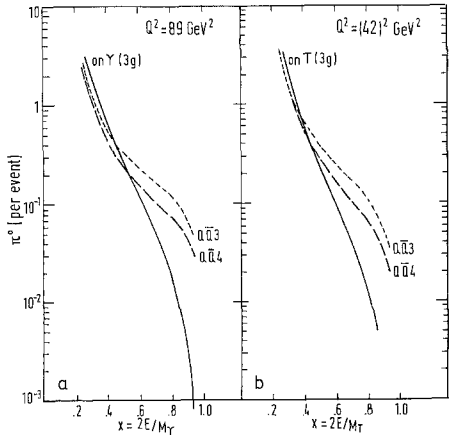

Fig. 9. Neutral pions per event, on and off the quarkonium resonances. Parameters are the same as in Fig. 8

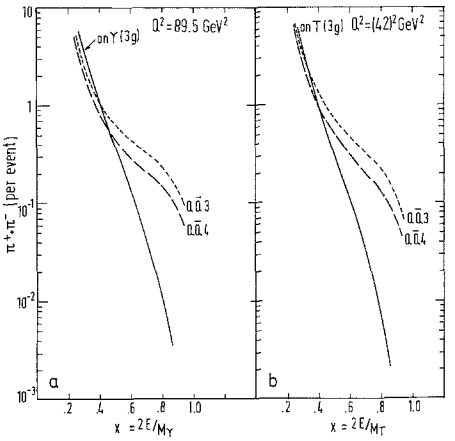

Fig. 10. Charged pions per event, on and off the quarkonium resonances. Parameters are the same as in Fig. 9

conference proceedings [3], which give an integrated number of baryons per event. This is because we cannot calculate down to very small values of x and have any confidence in the results. The main problem here is that the kinematic corrections due to the masses of the baryons are not present in our formalism, and we don't completely understand how they should be incorporated. If one simply guesses that the curve must turn over somehow near small x, the integral of the "on resonance" curve in Fig. 7a will come to to about 0.28, not inconsistent with the value given in [3]. (Needless to say, with the present set of approximations we are unable to produce different values for the different excitations of the heavy quark-antiquark bound state.)

The curves in Fig. 7 may be moved up and down by changing the value of R_B in the recombination function. Such adjustments will also change the relative position of the proton curve in Fig. 11. We expect that when enough data are available to justify such an adjustment, the value of R_B will not change from our value of 27/4 by much more than a factor of 2.

The results for the mesons are similar, except that the dominance of the "on resonance" events at small x is not nearly so marked. This is consistent with the data reported in [2] and [27].

In Figs. 7–10 two off-resonance curves are shown, labelled $Q\bar{Q}3$ and $Q\bar{Q}4$. The difference lies in the number of quarks produced at the photon vertex which are "jetting". In $Q\bar{Q}3$, only the up, down and strange quarks produce jets; in $Q\bar{Q}4$ the charmed quark is also assumed to produce a jet. The QCD evolution of all these jets uses only three flavors of quarks; i.e. the gluon can split only into $u\bar{u}$, $d\bar{d}$ and $s\bar{s}$ pairs. We regard it as quite unlikely that $c\bar{c}$ pairs are produced in the jet evolution up through the present measured range.

At the upsilon it is likely that $Q\bar{Q}3$ is more relevant than $Q\bar{Q}4$, at least for the baryon production. At the toponium, it seems reasonable to have at least four flavors jetting. (The possible inclusion of the fifth flavor, as shown in Fig. 12, makes very little difference).

Because the production mechanism of both baryons and mesons in this model at low x arises predominantly from the production and "conversion" of multiple gluons, the number produced per event, as shown in Figs. 7–10, is not greatly affected by the number of jet flavors even though the overall cross section of course increases as more flavors are taken into account. At large x, the inclusion of flavors like charm which do not directly contribute quarks to the produced particle leaves the absolute yields unchanged (see Fig. 12); hence the number per event is reduced.

Those flavors which are produced and contributing to the hadron cross section but not "jetting" will of course decay weakly, providing additional mesons and perhaps protons. Complete comparison with the data will require that these decays be modelled and added to the calculations here.

V. Summary and Conclusions

We have studied baryon and meson production in gluon jets, using a form of the jet calculus to generate parton distributions within the jet and the recombination model to package these into hadrons. All our parameters for both the mesons and the baryons $(\Lambda, (Q_0^2)_B, R_B, (Q_0^2)_M, R_M)$ are selected to make predictions consistent with data coming from quark jets; hence within this framework the gluon jet fragmentation functions are completely determined.

Because our gluon fragmentation function into baryons is larger than the quark fragmentation at low x, we predict more low energy baryons on the Υ than in adjacent parts of the e^+e^- continuum. In this our results agree with those of the Lund group [8] and Hoffmann [10], who had different approaches.

Within our framework, our expression for baryon production is in a very nonasymptotic region in Q^2. It remains to be seen whether this is a reasonable approach. However, as we stress in [12], we reproduce many features of the present data (leading quark effect, possible rise with Q^2 of the number of baryons, etc.). See Appendix C for a detailed discussion of the Q^2 dependence of this type of model. We are planning to recalculate the quantities studied here and in [11] and [12] by use of an improved jet calculus [16, 20]. In this other method, colorless clusters of quarks and gluons are produced and these then decay phenomenologically into the observed hadrons. While this approach potentially overcomes some of the theoretical limitations to our present calculation, it has the disadvantage that the naive but practical recombination model must be replaced by a potentially more complicated cluster decay function.

Acknowledgements. Both authors would like to thank the theory group at DESY for their hospitality while this work was being done. One of us (R.M.) wishes to thank NSERC of Canada for a Summer Research Fellowship. LMJ would also like to thank the CERN theory group for the opportunity to visit there during early stages of the calculations. Discussions with many physicists have improved our understanding of jet physics. In particular we would like to thank O. Nachtmann, F. Gutbrod, G. Veneziano, D. Amati, A. Bassetto, G. Marchesini, U. Sukhatme and M. Teper for illuminating discussions.

Appendix A

We present in Fig. 11 our predictions for $e^+e^- \to \pi^{+-}$, π^0, K^0, and $p+\bar{p}$ at $Q^2 = 1{,}089\ \mathrm{GeV}^2$. These should be compared with the Tasso data shown in Fig. 4 of [24]. Since many of these data are plotted in Appendix B, we do not reproduce the Tasso plot here. The main features of this data which interest us here are:

- The large x cross sections for pions, kaons, and lambdas are more or less parallel
- The lambda cross sections are about a factor two smaller than the kaon cross sections

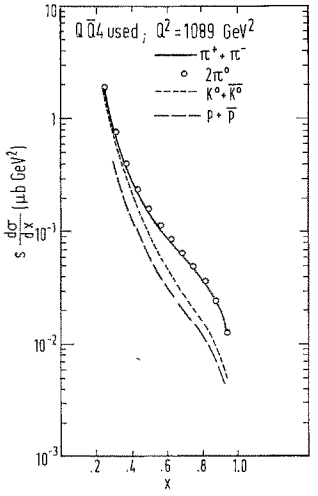

Fig. 11. Predictions at $Q^2 = 1{,}089\ \mathrm{GeV}^2$ for the meson and proton plus antiproton production in e^+e^- annihilation using the parameters of Fig. 2 for the baryons and Fig. 5 for the mesons. The option $Q\bar{Q}4$ (four flavors of quarks are making jets, but only 3 flavors are active in the evolution of the jets) is used

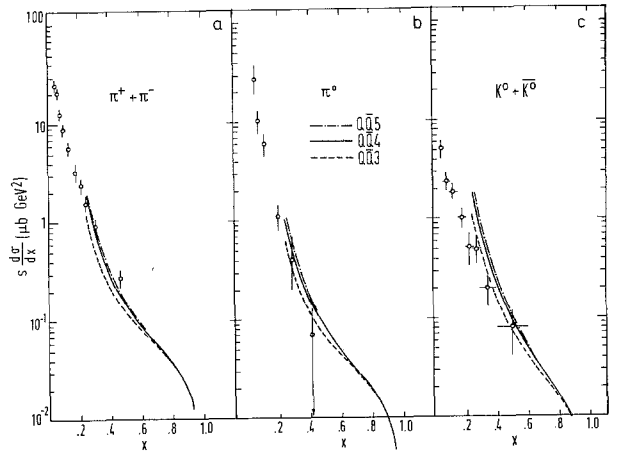

Fig. 12a–c. The various options $Q\bar{Q}3$, $Q\bar{Q}4$ and $Q\bar{Q}5$ are compared with recent Petra data using the parameters $Q_0^2 = 0.2\ \mathrm{GeV}^2$, $\Lambda = 0.2$ GeV, and $R_M = 1$. All curves have been calculated for $Q^2 = 1{,}089\ \mathrm{GeV}^2$. **a** Charged pions; the data shown are Tasso data at $Q^2 = 1{,}156\ \mathrm{GeV}^2$ [21]; **b** neutral pions; the data shown are Cello data at $Q^2 = 1{,}089\ \mathrm{GeV}^2$ [22]; **c** neutral kaons; the data shown are TASSO data at $Q^2 = 1{,}089\ \mathrm{GeV}^2$ [23]

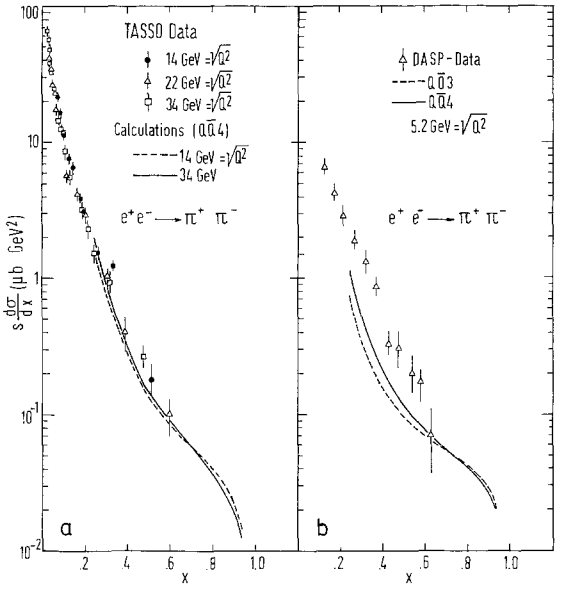

Fig. 13a and b. Energy dependence of charged pion production using the same parameterization as in the other meson graphs. **a** Comparison with Tasso data [21] using the option $Q\bar{Q}4$ (see text); **b** comparison with DASP data [24] showing the two options $Q\bar{Q}3$ and $Q\bar{Q}4$ (see text)

• The charged pion yields are almost exactly twice the neutral pion yields.

Since we expect there to be somewhat more protons than lambdas, the overall normalization of the proton curve in our calculation seems about right. As discussed in the text this can be adjusted somewhat once more data is known.

Also, we see that twice the pi zero cross section is almost exactly equal to the charged pion cross section; and that all the curves have a similar shape at large x.

Appendix B

Here we compare our parameterization $Q_0^2 = 0.2\ \mathrm{GeV}^2$, $\Lambda = 0.2$ GeV, $R_M = 1$ with available data for meson production in e^+e^- annihilation. The Teper probability argument [17] applied to the recombination function of (2.4) would allow a maximum value $R_M = 4$. Older fits [11, 13] to the π^+ inclusive spectrum found $R_M = 1$ gave a good fit, and we continue to find this reasonable. In Fig. 12, results are presented for various different numbers of flavors of jets produced at the photon vertex; in all cases only three flavors are assumed to take part in the QCD evolution of the jet. Due to the small electric charge of the b quark, its inclusion is almost irrelevant.

Notice in Fig. 12c that the fit to the neutral kaon data is not as good as the fit to the pion data in the first two figures. There are two adjustments possible to the model, both of which are in the right direction to correct this discrepancy. The first is that our Q_0^2 of $0.2\ \mathrm{GeV}^2$ is a little small for the kaons; we might expect a Q_0 at least as big as the kaon mass. As can be seen from Fig. 3 (or similar graphs in our previous papers), increasing this parameter will tend to pull the curve down at small x, thus decreasing its slope. The other likely adjustment is the inclusion of mass corrections at the end of the cascade where gluon splittings occur. These would tend to decrease the amount of strange quarks produced compared with the number of nonstrange quarks.

Another important effect which matters at small x is mass corrections due to the mass of the produced particle. This will affect the proton production as well. At present we do not know how to incorporate these effects into our calculation, so we put most emphasis on the behavior at larger x where the calculation is more accurate.

In Fig. 13 we address the problem of the energy dependence of the predictions. The Tasso data is plotted in Fig. 13a, along with our $Q\bar{Q}4$ predictions. With the present choice of parameters, the calculations show very little change with energy in this region, this is consistent with the data. In Fig. 13b we compare with the lower energy DASP data. This data has a 15% normalization uncertainty; however our predictions lie a bit below the data even if this is allowed for.

Appendix C

The purpose of this Appendix is to discuss the relation of our work to the similar calculation of

Eilam and Zahir (EZ) [25] and to discuss a number of the properties of the method, with emphasis on those which should be improved in better models.

Comparison With Eilam and Zahir

The work of these two authors is superficially very similar to ours in that they use the KUV jet calculus to generate a spray of partons which are then recombined. Since those authors have much smaller values for their fragmentation functions in general, and since their graph comparing the size of the gluon and quark fragmentation functions looks quite different from our Fig. 2c, we feel some discussion is in order.

There are, unfortunately, many differences in the two actual calculations.

• First, EZ use a different recombination function,

$$19.9\,\frac{(x_1x_2)^{1.65}x_3^{1.35}}{x^{4.65}}\,\delta(x_1+x_2+x_3-x) \qquad \text{(C.1)}$$

which not only has a different power behavior in the individual x_i but also is normalized according to a different prescription.

• Second, they use different values for the parameters Q_0^2 and Λ in the jet calculus. (They have $Q_0^2=0.64\,\mathrm{GeV}^2$, $\Lambda=0.65$ GeV)

• Thirdly, instead of performing the full integrals in (2.1), they cut off the integrals at an upper $Q^2=30\,\mathrm{GeV}^2$; the intent of this was to restrict the relative transverse momentum of the quarks.

Let us deal with these differences in turn. Because we invert moments with Yndurain's method, we are not particularly well equipped to deal with noninteger powers in the recombination function so it is not easy for us to exactly duplicate their work. We can, however, compute the results for the two functions

$$\frac{27}{4}\,\frac{x_1x_2x_3}{x^3}\,\delta(x_1+x_2+x_3-x) \quad (n=1) \qquad \text{(C.2)}$$

and

$$\frac{(27)^2}{4}\left(\frac{x_1x_2x_3}{x^3}\right)^2\delta(x_1+x_2+x_3-x) \quad (n=2). \qquad \text{(C.3)}$$

The results are shown in Fig. 14. We see that the values of the answers are reduced by about a factor of 4 with our normalization prescription for the recombination function. If we had instead used the valon model prescription for normalization [26], we would have 120 for the normalization in (C.3) instead of $(27)^2/4$. Thus the overall answers would be reduced by a factor of about 6 (i.e. Our $n=1$ answers with our normalization of 27/4 would be a factor 6 larger than $n=2$ answers with the valon model prescription). Since the EZ function is partway between $n=1$ and $n=2$, we might expect an overall factor of not more than 10 difference between our calculation and theirs from the different power and normalization prescriptions.

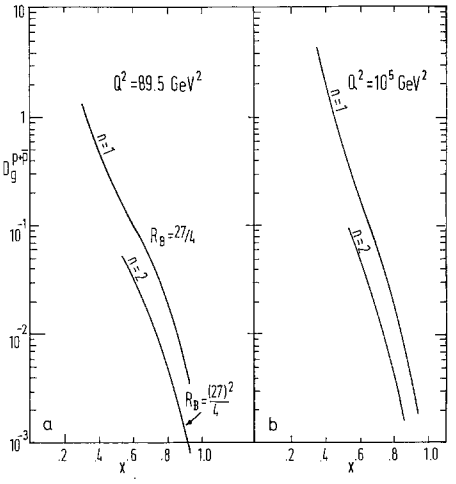

Fig. 14a and b. Dependence of the gluon fragmentation function into protons on the power n of the recombination function

$$R_n\left(\frac{x_1x_2x_3}{x^3}\right)^n\delta(x_1+x_2+x_3-x).$$

All curves are calculated with $Q_0^2=2\,\mathrm{GeV}^2$, $\Lambda=0.2$ GeV. With our normalization prescription $R_1=27/4$; $R_2=27^2/4$. **a** $Q^2=89.5\,\mathrm{GeV}^2$; **b** $Q^2=10^5\,\mathrm{GeV}^2$

The effect of using the Oregon values for Q_0^2 and Λ is to make the baryon results "asymptotic" at a much lower Q^2 than is the case with our values $Q_0^2=2\,\mathrm{GeV}^2$ and $\Lambda=0.2$ GeV (if no cutoff is used in the jet calculus). This is shown in Fig. 12 of [12]. Actually, no figures are necessary since the jet calculus answer is a function of only $Y-Y_0$, and it is easy to compute that with

$$Y-Y_0=\frac{1}{2\pi b}\cdot\ln[(1+\alpha_0 b\ln Q^2/\Lambda^2)/(1+\alpha_0 b\ln Q_0^2/\Lambda^2)]$$

the value of Q^2 corresponding for our calculation to their value of 900 is about 2×10^{23}. As a practical matter, therefore, we are always operating in the nonasymptotic region of our expression. This may be objectionable on aesthetic grounds.

Finally, the cutoff placed on the y integrals by Eilam and Zahir should have the effect of giving their results exact Altarelli-Parisi behavior, since for all Q^2 above $30\,\mathrm{GeV}^2$ their expression can be written in the form

$$D_i^p(Q^2,n)=D_{ji}(Y-Y(30),n)D_j^p(30,n). \qquad \text{(C.4)}$$

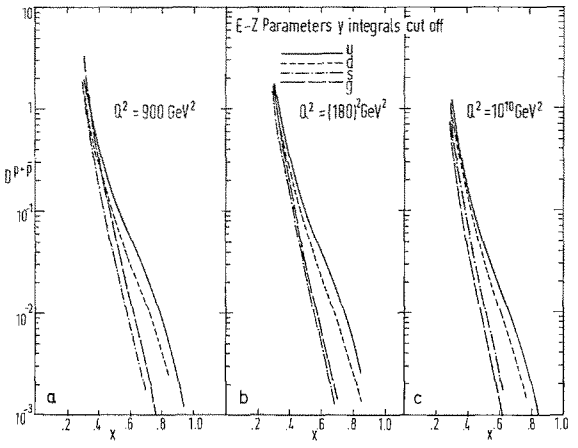

Fig. 15a–c. To prepare this figure, we computed the full jet calculus at $Q^2=30\,\mathrm{GeV}^2$ with our form of the recombination function and the Eilam-Zahir parameterization $R_B=2$, $Q_0^2=0.64\,\mathrm{GeV}^2$, $\Lambda=0.65\,\mathrm{GeV}$. We then used the Altarelli-Parisi equations to evolve these values to larger Q^2. This should be equivalent to the Oregon group's technique of cutting off the y integrals. **a** $Q^2=900\,\mathrm{GeV}^2$ (compare Fig. 3 of [25]); **b** $Q^2=(180)^2\,\mathrm{GeV}^2$ (compare Fig. 4 of [25]); **c** $Q^2=10^{10}\,\mathrm{GeV}^2$

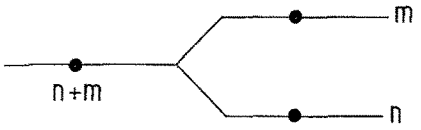

Fig. 16. The jet calculus preserves "moment" at the vertices

Unfortunately the Q^2 dependence of their results at small x is not consistent with this.

To get some idea of what their results would look like with our (Yndurain)inversion technique, (or what our results would look like with a cutoff on the y integrals) we have computed the moments at $Q^2=30\,\mathrm{GeV}^2$ and have evolved these values with the Altarelli-Parisi equations, using our recombination function (2.3) but their Q_0^2, Λ and the valon normalization $R_B=2$. This involves no approximations. Then we inverted them with the Yndurain technique. The results are shown in Fig. 15. Comparing with Figs. 3 and 4 of [25], we see that

- At large x, where they believe their method to be more accurate, and where our inversion technique is certainly most accurate, our results differ from theirs by a factor of about 10^2 (far greater than the factor expected from power differences)
- For the two Q^2 values they plot, $Q^2=900$ and $Q^2=(180)^2\,\mathrm{GeV}^2$, the gluon function is relatively larger in our calculation than in theirs
- We must go to quite large Q^2 (we show $Q^2=10^{10}$ here) to obtain a gluon function which lies below the quark function everywhere above $x=0.3$. In their Figs. 3 and 4 the gluon function is depicted as lying below the quark function at all x.

In summary, we do not understand the size of their answers. When we reproduce their technique as closely as we can, we find much larger values. Also we find that in the energy range they covered, the gluon jets are relatively more important than they show.

General Properties of the Method; Places for Improvment

Q^2 Dependence. If we begin by considering a recombination function for mesons of the general form

$$R_M\left(\frac{x_1x_2}{x^2}\right)^{NN}\delta(x_1+x_2-x) \tag{C.5}$$

where NN is some integer power, we see that the moments of the recombined fragmentation function for mesons take the form [11]

$$D_i^M(N,Y)=\int_{Y_0}^{Y} D_{ji}(N,Y-y)f_j^N(y)\,dy \tag{C.6}$$

with

$$f_j^N(y)=\sum_{a_1a_2b_1b_2}\sum_{m=0}^{N-2NN}\binom{N-2NN}{m}C_{a,a_2\to M}\cdot D_{a_1b_1}^{N-NN-m}(y-Y_0)D_{a_2b_2}^{m+NN}(y-Y_0)P_{j\to b_1b_2}^{N-NN-m,m+NN}. \tag{C.7}$$

Of course there is a similar but much more complicated expression for the baryons [12].

If we go into a representation where the parton propagators D_{ij} are diagonal, contributions to (C.6) from the diagram of Fig. 16 will have the form

$$D(n+m,Y)\sim e^{(\lambda_{m+}\lambda_n)(Y-Y_0)}-e^{\lambda_{m+n}(Y-Y_0)}. \tag{C.8}$$

As long as n and m are greater than 1, there is always one $n+m$ eigenvalue such that $\lambda_{n+m}>\lambda_n+\lambda_m$. In this case, as $Y-Y_0$ gets large, the contributions to the $n+m$'th moment will asymptotically have the canonical Altarelli-Parisi behavior in Q^2.

Provided the recombination function power NN is 2 or greater, no first moments will contribute to the sums in (C.7) at all and in principle one has ensured that asymptotically the Q^2 dependence will be of this simple form.

However, as we show in Fig. 17, where we plot the Q^2 dependence of the $D_g^{p+\bar{p}}$ moments for the $NN=2$ case, asymptopia will never be attained for our parameterization. None of the moments falls nearly as fast as one would expect from the Altarelli-Parisi eigenvalues for the appropriate total moment number values. The reason for this is simple: $Y-Y_0$ is never very big, and the actual Q^2 dependence of the moments comes from the cancellation between the terms of (C.8). (Doubtors should plot the function $\exp(-3x)-\exp(-5x)$, and recall that with our pa-

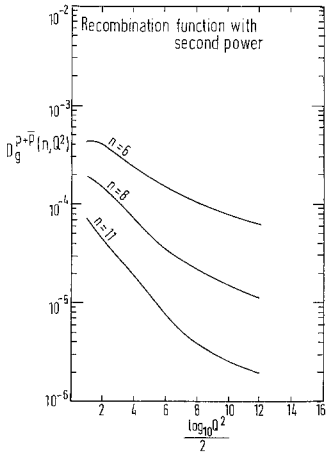

Fig. 17. Q^2 dependence of the moments of $D_g^{p+\bar{p}}$ computed with the recombination function

$$\frac{(27)^2}{4}\left(\frac{x_1x_2x_3}{x^3}\right)^2\delta(x_1+x_2+x_3-x)$$

($Q_0^2=2$ GeV^2, $\Lambda=0.2$ GeV). Although in principle these moments behave asymptotically like solutions of the Altarelli-Parisi equations, in practice asymptopia is not reached at reasonable Q^2

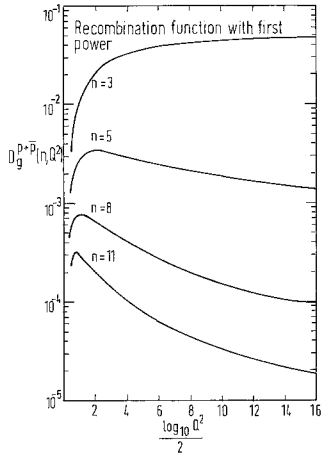

Fig. 18. Q^2 dependence of the moments of $D_g^{p+\bar{p}}$ computed with recombination function

$$\frac{27}{4}\left(\frac{x_1x_2x_3}{x^3}\right)\delta(x_1+x_2+x_3-x)$$

rameters $Y-Y_0$ at $Q^2=10^6$ is 0.32 for the baryon case and 0.51 for the meson case).

This determination of the Q^2 behavior of the moments by cancellation between the terms holds also for the $NN=1$ case - the case used for the calculations presented in this paper. In this case, there is a potential problem of principle because the $n=1$ moments have a zero eigenvalue, and in the terms where this occurs one has $\lambda_{n+m}<\lambda_n+\lambda_m$. These contributions therefore will not have Altarelli-Parisi behavior asymptotically as $Y-Y_0$ becomes large.

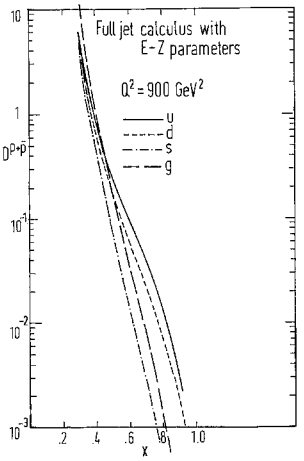

Fig. 19. Computation of the full jet calculus for our recombination function

$$R_B\frac{x_1x_2x_3}{x^3}\delta(x_1+x_2+x_3-x)$$

using the Eilam-Zahir parameterization $R_B=2$, $Q_0^2=0.64$, $\Lambda=0.65$. Results are presented for $Q^2=900$ GeV^2. Compare Fig. 15a of this paper and Fig. 3 of [25]

As shown in Fig. 18, all the moments ultimately decrease with Q^2 except the $n=3$ moment, which can have three zero eigenvalues contributing for the baryon case (or two for the meson case). Furthermore, the rate of decrease of these $n\neq 3$ moments with Q^2 is similar to that of the $NN=2$ moments.

In the inversion routine, the $n=3$ moment contributes only to the lowest point in x (0.3077 for our baryon case). Hence if this point is excluded, the contribution at each of the higher points $(J+1)/(NMOM+2)$ is obtained from terms each of which has decreasing behavior with Q^2 (see (C.9) below). In Yndurain's method, the moments contribute with alternating signs to the value at each x point (except for the point at the largest x, where only one moment contributes). The increasing values with Q^2 of our calculations at small x are due partly to this cancellation between the decrease of various moments and partly (at lower Y) to the increase of terms like (C.8) from zero at $Y=Y_0$.

Some idea of the practical difference between our full jet calculus and the cutoff version can be got by comparing Fig. 15a with Fig. 19. These are computed with the EZ parameters; with our values of Q_0^2 and Λ the difference will be much more marked because of the growth shown in Fig. 2a.

Inversion Method

The values of functions of x presented in this paper have been obtained from the basic Yndurain for-

mula [14].

$$F\left(\frac{J+1}{NMOM+2}\right)\approx\frac{(NMOM+1)!}{J!}\cdot\sum_{l=0}^{NMOM-J}\frac{(-)^l\mu_{J+l}}{l!(NMOM-J-l)!} \quad \text{(C.9)}$$

where

$$\mu_{J+l}=\int_0^1 x^{J+l}F(x)dx.$$

We do not use the "correction term", which we find frequently makes agreement with the true function worse.

The simple formula (C.9) gives very good reproduction of functions at large x; at small x on test functions with shapes similar to those of the experimental fragmentation functions, (C.9) may overestimate the values at small x by as much as 20 or 30%. However, we have never found a case in which it underestimates the function in this region. Hence we believe the relative sizes of the curves plotted are approximately correct despite potential problems with the method.

As mentioned above, the alternative method used by Eilam and Zahir, that of fitting the large n moments with moments of a function in x designed to have reasonable behavior at large x, apparently has the property that it treats the small x points incorrectly. Our method is also inaccurate in the small x region, but we believe the inaccuracies to be smaller.

References

1. K. Konishi, A. Ukawa, G. Veneziano: Phys. Lett. **78B**, 243 (1978); Nucl. Phys. **B157**, 45 (1979)
2. H. Albrecht et al.: Phys. Lett. **102B**, 291 (1981)
3. R.D. Schamberger: Proceedings of the 1981 International Symposium on Lepton and Photon Interactions at High Energies, p. 52; A. Silverman: ibid. p. 158
4. G. Schierholz, M. Teper: Z. Phys. C - Particles and Fields **13**, 53 (1982)
5. D. Wegener: Evidence for gluon effects in high p_t events. Talk presented at DESY QCD Workshop, 1981; P. Hanke: Talk presented at XVIIth Rencontre de Moriond
6. F. Gutbrod: Review of baryon production in hard processes. Talk given at the IV International Warsaw Symposium on Elementary Particles, 1981
7. S. Ritter, J. Ranft: Acta Phys. Polon. **B11**, 259 (1980); A Bartl, H. Fraas, W. Majerotto: Quark and diquark fragmentation into mesons and baryons. Vienna preprint UWThPh-81-28; U.P. Sukhatme, K.E. Lassila, R. Orava: Fermilab Pub 81/20-THY; U.P. Sukhatme: Z. Phys. C - Particles and Fields **2**, 321 (1979)
8. B. Andersson: LU TP 81-7; B. Andersson, G. Gustafson, T. Sjostrand; LU TP 81-3; B. Anderson, G. Gustafson, G. Ingelman, T. Sjostrand: LU TP 81-6. To be published in Z. Phys. C - Particles and Fields
9. T. Meyer: Z. Phys. C - Particles and Fields **12**, 77 (1982)
10. W. Hoffmann: Z. Phys. C - Particles and Fields **10**, 151 (1981)
11. L.M. Jones, K.E. Lassila, U. Sukhatme, D.E. Willen: Phys. Rev. **D23**, 717 (1981)
12. R. Migneron, L.M. Jones, K.E. Lassila: Phys. Lett. **114B**, 189 (1982); R. Migneron, L.M. Jones, K.E. Lassila: Production of protons and lambdas in e^+e^- jets from jet calculus and the recombination model, (to appear in Phys. Rev. D)
13. V. Chang, R.C. Hwa: Phys. Rev. Lett. **44**, 439 (1980)
14. F.J. Yndurain: Phys. Lett. **74B**, 68 (1978)
15. K. Koller, T. Walsh: Nucl. Phys. **B140**, 449 (1978); J. Körner, D.H. Schiller: DESY 81-043
16. D. Amati et al.: Nucl. Phys. **B173**, 429 (1980)
17. M.J. Teper: Rutherford Preprint RL-78-022/A, 1978 (unpublished)
18. L.M. Jones: DESY 81-085. Phys. Rev. **D26**, 706 (1982)
19. R. Felst: Proceedings of 1981 International Symposium on Lepton and Photon Interactions at High Energies, p. 52
20. A. Bassetto, M. Ciafaloni, G. Marchesini: Nucl. Phys. **B163**, 477 (1980)
21. TASSO collaboration et al.: Charged pion production in e^+e^- annihilation at 14, 22 and 34 GeV c.m. energy. DESY 82-009
22. CELLO collaboration H.J. Behrend et al.: Z. Phys. C - Particles and Fields **14**, 189 (1982)
23. TASSO collaboration et al.: Production in e^+e^- annihilation at 33 GeV centre of mass energy. DESY 81-039
24. R. Brandelik et al.: Nucl. Phys. **B148**, 189 (1979)
25. G. Eilam, M.S. Zahir: to appear in Phys. Rev. D
26. R.C. Hwa: Phys. Rev. **D22**, 1593 (1980)
27. L. Criegee, G. Knies: Phys. Rep. **83**, (1982)